Vibration-Theoretic Approach to Vulnerability Analysis of Nonlinear Vehicle Platoons

Pengcheng Wang, Xinkai Wu, Xiaozheng He

***Abstract*—This research explores the inherent vulnerability of nonlinear vehicle platoons characterized by the oscillatory behavior triggered by external perturbations. The perturbation exerted on the vehicle platoon is regarded as an external force on an object. Following the mechanical vibration analysis in mechanics, this research proposes a vibration-theoretic approach that advances our understanding of platoon vulnerability from two aspects. First, the proposed approach introduces damping intensity to characterize vehicular platoon vulnerability, which divides platoon oscillations into two types, *i.e.*, underdamped and overdamped. The damping intensity measures the platoon's recovery strength in responding to perturbations. Second, the proposed approach can obtain the resonance frequency of a nonlinear vehicle platoon, where resonance amplifies platoon oscillation magnitude when the external perturbation frequency equals the platoon's damping oscillation frequency. The main contribution of this research lies in the analytical derivation of the closed-form formulas of damping intensity and resonance frequency. In particular, the proposed approach formulates platoon dynamics under perturbation as a second-order non-homogeneous ordinary differential equation, enabling rigorous derivations and analyses for platoons with complicated nonlinear car-following behaviors. Through simulations built on real-world data, this paper demonstrates that an overdamped vehicle platoon is more robust against perturbations, and an underdamped platoon can be destabilized easily by exerting a perturbation at the platoon's resonance frequency. The theoretical derivations and simulation results shed light on the design of reliable platooning control, either for human-driven or automated vehicles, to suppress the adverse effects of oscillations.**

***Index Terms*—Vehicle Platoon; Vulnerability; Mechanical vibration theory; Damping characteristics**

I. INTRODUCTION

Driving in smooth traffic flow enhances travel comfort, reduces fuel consumption and emissions, and mitigates collision risks. Unfortunately, traffic oscillation, or stop-and-go traffic, occurs frequently, particularly in congested traffic [1]. This phenomenon is likely to elicit a variety of adverse effects, such as increased travel delay and crash risk, driving discomfort, and extra fuel consumption and pollution [2, 3]. To mitigate these adverse effects, extensive studies seek to identify and analyze the contributing factors and resulted impacts on traffic stream using stability analysis [4].

The aim of stability or instability analysis is to describe whether a perturbation decays or amplifies along with a string of vehicles [5-7]. Researchers, such as Gratzer *et al.* [8], have developed robust methods for ensuring string stability in automated vehicle platoons through predictive control. Vegamoor *et al.* [9] explored string analysis in connected-vehicle platoons under lossy V2V communication. Monteil *et al.* [10] discussed the impact of the heterogeneity of vehicles on string stability. String stability is considered a performance-oriented approach, which ensures that the spacing errors generated within the platoon are not amplified as they propagate downstream [11]. Moreover, Feng *et al.* [12] presented different definitions of string stability and analysis methods.

However, such analysis is unable to reveal the features inherent in vehicle platoons, *e.g.*, damping characteristics. Gong *et al.* [13] found that for a stable vehicle platoon system, the oscillations in the vehicle platoon should be damped when they reach the tail of the platoon. Hajidavalloo *et al.* [14] proposed using damping characteristics to capture the vehicle's tendency to resist large speed variance. Hence, in addition to stability and instability analyses, the damping behavior of vehicle platoons is another major concern in analyzing vehicle platoon vulnerability when facing perturbations.

Vulnerability is a crucial concept being studied in diverse fields. As suggested by Chen *et al.* [15], vulnerability is subject to perturbation and thus could cause the system to collapse. In transportation, vulnerability is defined as the susceptibility to incidents that can cause considerable serviceability reduction in transportation network [16]. Growing research has identified vehicles' vulnerabilities and analyzed potential impacts [17]. For example, Ploeg *et al.* [18] claimed that Cooperative Adaptive Cruise Control (CACC) is vulnerable to communication impairments such as packet loss, in which case it would effectively degrade to conventional Adaptive Cruise Control (ACC). Meanwhile, Zhou *et al.* [19] found that due to the vulnerability of the communication process, the cyber-attack may be launched by hackers. Hence, vulnerability is an inherent characteristic of the vehicle platoon. The platoon with

This work was supported in part by the Young Scientists Fund of the National Natural Science Foundation of China (52002013), National Natural Science Foundation of China (52172376) and the U.S. National Science Foundation (CMMI-2047793). *(Corresponding author: Xiaozheng He)*

Pengcheng Wang is with School of Cyber Science and Technology, Beihang University, Beijing, China (e-mail: pcwang@buaa.edu.cn).

Xinkai Wu is with School of Transportation Science and Engineering, Beihang University, Beijing, China (e-mail: xinkaiwu@buaa.edu.cn).

Xiaozheng He is with Department of Civil and Environmental Engineering, Rensselaer Polytechnic Institute, Troy, NY, United States (hex6@rpi.edu).

different control models and with/without communication schemes has different vulnerabilities. However, most studies focus on assessing the consequences of vulnerable systems without much attention paid to inherent attributes leading to system vulnerability.

To advance our understanding of platoon vulnerability to more generic circumstances, this study proposes to explore a platoon's vulnerability using the mechanical theory of the forced vibration of a damped system [20], where an external force exerted on an object will cause vibrations in the system. In line with mechanical vibration theory, perturbations can be regarded as external forces causing a vehicle platoon to oscillate. If a perturbation (or force) is imposed on a vehicle (or an object), the vehicle state (or object) will oscillate (or vibrate); and once the perturbation (or force) stops, the oscillating vehicle platoon (or vibrating object) restores its equilibrium state. Hence, a tiny but sustained perturbation can cause severe impacts on a vehicle platoon, calling for in-depth analyses of vehicle platoon vulnerability. Furthermore, this research provides detailed analyses and theoretical proofs on deriving damping characteristics, *i.e.*, damping intensity and resonance frequency, and how resonance phenomena could occur in a perturbed travel environment.

In summary, the main contributions of this paper include the following three aspects. First, this research analyzes the vehicle platoon vulnerability by modeling the system as a second-order non-homogeneous ordinary differential equation, incorporating a generic platoon control model with periodic perturbation. Second, the proposed approach provides closed-form formulas for the damping intensity and resonance frequency that are new metrics for vulnerability analysis of vehicle platoon and can be used to analyze the vulnerability of any vehicle platoon, regardless of whether the underlying vehicle dynamics model is linear or nonlinear. These closed-form formulas are particularly useful for protecting platoons under automated control, such as adaptive cruise control systems. Third, the research evaluates the effectiveness of the proposed approach, which illustrates that the periodic perturbation with a frequency equal to the platoon's resonance frequency will degrade the vehicle platooning reliability and amplify oscillation amplitude. The damping intensity and resonance frequency derived from the proposed approach are powerful measures to analyze vehicle platoon vulnerability and protect the vehicle platoon from adverse perturbations.

In the remainder of this paper, Section II derives closed-form formulas of damping intensity and resonance frequency for characterizing vehicle platoon oscillations. Section III elaborates on vehicle platoon vulnerability by applying the proposed analysis approach to a nonlinear vehicle dynamics model. Numerical studies are carried out to demonstrate the theoretical properties in Section IV, followed by the section summarizing findings and future research directions.

II. Vibration-Theoretic Approach

This section analytically derives damping oscillation characteristics of vehicle platoons. Section 2.1 introduces a generic vehicle dynamics model with no perturbation. Section 2.2 reformulates the car-following model into a vibration expression in the form of a *homogeneous* ordinary differential equation (ODE) by employing the mechanical vibration theory. The reformulated ODE enables us to solve for the damping oscillation frequency and damping intensity analytically. The closed-form solutions to the ODE establish a rigorous relationship between damping intensity and platoon's oscillation patterns. Section 2.3 extends the analysis to a vehicle platoon under periodic perturbation, which is formulated as a second-order *non-homogeneous* ODE. The derived closed-form solutions to the non-homogeneous ODE establish the theoretical foundation for addressing the occurrence of resonance phenomenon and helps to explore the effect of perturbation frequency on vehicle platoon oscillation.

A. Car-following model

To enhance the transferability of our proposed approach, This study considers a vehicle platoon consisting of *N* identical members indexed by $n = 1, \cdots, N$.

To analyze traffic dynamics, various car-following models have been developed since the pioneering work [21]. A typical stimulus-response car-following model has a generic form:

$$\begin{aligned} \dot{x}_n(t) &= v_n(t), \\ \dot{v}_n(t) &= f\left(s_n(t), v_n(t), \Delta v_n(t)\right). \end{aligned} \tag{1}$$

where $s_n = x_{n-1} - x_n - l_{n-1}$ is the space gap and $\Delta v_n = v_{n-1} - v_n$ is the velocity difference between two consecutive vehicles. Define v^{e} and s^{e} as uniform speed and gap, respectively, μ and y as the offsets of the speed and space gap with respect to v^{e} and s^{e}, respectively, *i.e.*,

$$v_n = v^{\mathrm{e}} + \mu, \;\; s_n = s^{\mathrm{e}} + y. \tag{2}$$

In a steady state, each following vehicle has the same speed and space gap. Hence, the second equation of Eq. (1) is deduced as $f(s^{\mathrm{e}}, V(s^{\mathrm{e}}), 0) = 0$ at equilibrium. When a perturbation occurs, vehicles start oscillating [22]. This is Similar to a spring-mass system: after removing an external force, the mass vibrates from its equilibrium position. Due to the damper force, the mass eventually recovers its steady state. To this end, the next section will employ the mechanical theory to investigate the platoon's vulnerability.

B. Damping oscillation analysis without perturbation

This section develops the damping characteristics of platoons without perturbations by applying the unforced damping vibration theory. For a spring-mass system, k denotes the recovery constant and d denotes the damper coefficient that linearly restraints the mass movement. The generic dynamic model of the spring-mass system is expressed as the following homogeneous ODE [23]:

$$\ddot{x}(t)+\frac{d}{m}\dot{x}(t)+\frac{k}{m}x(t)=0, \tag{3}$$

where $x(t)$, $\dot{x}(t)$, and $\ddot{x}(t)$ represent the position, speed and acceleration of the mass, respectively.

Eq. (3) is a common expression of the spring-mass system [24]. As discussed, vehicle platoon oscillations are like mechanical vibrations. Hence, this study attempts to analyze the platoon's oscillations using mechanical vibration theory. Our previous study [25] has introduced Lemma 1 below, which describes the oscillation of platoon vehicles following a second-order differential equation in the form of Eq. (3).

Lemma 1. The vehicle platoon's oscillation dynamics follow the second-order homogeneous ODE, *i.e.*,

$$\frac{d^2y}{dt^2}+2\omega_0\xi\frac{dy}{dt}+\omega_0^2y=0, \tag{4}$$

where $\xi=-\frac{1}{2}\left(f_n^v-f_n^{\Delta v}\right)\Big/\sqrt{\left|f_n^s\right|}$, $\omega_0^2=f_n^s$, $f_n^v=\left.\frac{\partial f}{\partial v_n}\right|_{(v^e,s^e)}$, $f_n^s=\left.\frac{\partial f}{\partial s_n}\right|_{(v^e,s^e)}$ and $f_n^{\Delta v}=\left.\frac{\partial f}{\partial \Delta v_n}\right|_{(v^e,s^e)}$.

In Lemma 1, notations ω_0 and ξ indicate the platoon's resonance frequency and damping intensity against perturbation. The ODE Eq. (4) can be solved by the characteristic equation method. The closed-form solutions, derived in Theorem 1, provide a rigorous way to analyze how the damping intensity affects the vehicles' oscillations.

Theorem 1. Let $y(0)$ and $\dot{y}(0)$ indicate the initial distance offset and velocity offset, respectively. The solution of Eq. (4) can be obtained in terms of different values of ξ:

(i) When $\xi<1$,

$$y(t)=Ae^{-\xi\omega_0 t}\sin\left(\omega_d t+\phi_d\right) \tag{5}$$

where $A=\sqrt{y(0)^2+\left(\frac{\dot{y}(0)+\xi\omega_0 y(0)}{\omega_d}\right)^2}$, $\phi_d=\tan^{-1}\left(\frac{y(0)\omega_d}{\dot{y}(0)+\xi\omega_0 y(0)}\right)$.

(ii) When $\xi=1$,

$$y=e^{-\xi\omega_0 t}\left(y_1e^{t\omega_0\sqrt{\xi^2-1}}+y_2e^{-t\omega_0\sqrt{\xi^2-1}}\right) \tag{6}$$

where $y_1=\frac{\dot{y}(0)+\left(\xi+\sqrt{\xi^2-1}\right)\omega_0 y(0)}{2\omega_0\sqrt{\xi^2-1}}$, $y_2=\frac{-\dot{y}(0)-\left(\xi-\sqrt{\xi^2-1}\right)\omega_0 y(0)}{2\omega_0\sqrt{\xi^2-1}}$.

(iii) When $\xi>1$,

$$y=e^{-\xi\omega_0 t}\left(y_1e^{t\omega_0\sqrt{\xi^2-1}}+y_2e^{-t\omega_0\sqrt{\xi^2-1}}\right) \tag{7}$$

where $y_1=\frac{\dot{y}(0)+\left(\xi+\sqrt{\xi^2-1}\right)\omega_0 y(0)}{2\omega_0\sqrt{\xi^2-1}}$, $y_2=\frac{-\dot{y}(0)-\left(\xi-\sqrt{\xi^2-1}\right)\omega_0 y(0)}{2\omega_0\sqrt{\xi^2-1}}$.

Appendix A provides proof of Theorem 1. For the spring-mass system, conditions $\xi<1$ and $\xi\geq 1$ characterize the underdamped and overdamped system, respectively. For a underdamped system, the mass vibrates back and force around the equilibrium; for an overdamped system, the mass hardly vibrates and converges to its equilibrium without overshoot. Applying this notion to a vehicle platoon, $\xi<1$ denotes that vehicles could oscillate reciprocally around the steady state, while $\xi\geq 1$ denotes that vehicles hardly oscillates and tend to stabilize rapidly. Hence, the vehicle platoon system with $\xi\geq 1$ could make the platoon suppress the oscillating effect caused by perturbations. This property helps to enhance platoon's reliability in a perturbed travel environment.

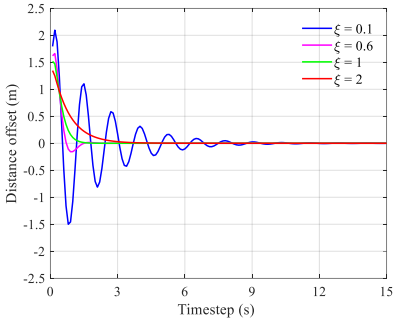

Fig. 1. Distance offset variations with different ξ

To illustrate the impacts of ξ on platoon's oscillations, a set of comparable oscillation curves can be constructed and analyzed as follows. Fig. 1 plots four curves when $\xi=0.1$, $\xi=0.6$, $\xi=1$ and $\xi=2$. Other parameters are the same, *i.e.*, $y(0)=1$, $\dot{y}(0)=1$ and $\omega_0=0.5$. This figure shows the decay tendency of the oscillation with different values ξ. The two curves with $\xi<1$ (*i.e.*, $\xi=0.1$ and $\xi=0.6$) present that the distance offset fluctuates around the equilibrium line (*i.e.*, y=0) and decays gradually. When $\xi\geq 1$ (*i.e.*, $\xi=1$ and $\xi=2$) the distance offset converges to the equilibrium state without overshoots. Hence, when a perturbation arises, an overdamped system can restore its equilibrium state without much oscillation compared to an underdamped system, implying a lower risk of disruption. This section presents a vulnerability analysis approach to vehicle platoon without perturbation. The next section will extend this approach to explore the vulnerability of vehicle platoons under perturbation.

C. Damping oscillation analysis with periodic perturbation

A perturbation on the vehicle platoon can be regarded as an external force exerted on a mechanical system. For simplicity, the perturbation is assumed to follow a periodic pattern, enabling us to derive closed-form solutions to the ODE. By introducing the external force to the vehicle platoon's oscillation dynamics, the right-hand side of the second-order ODE, *i.e.*, Eq. (4), cannot maintain zero, yielding a non-homogeneous ODE. The platoon oscillation characteristics under a periodic perturbation can be derived as follows.

Lemma 2. A vehicle platoon's oscillation dynamics under perturbation follow the second-order non-homogeneous ODE:

$$\frac{d^2y}{dt^2}+2\omega_0\xi\frac{dy}{dt}+\omega_0^2y=\mu(t), \tag{8}$$

where $\mu(t)$ represents a periodic external perturbation.

Proof. This Lemma is self-explanatory.

Note that the external force can be formulated as a Fourier series as a superposition of a series of sinusoidal and cosine functions. And any periodic functions can be transformed into a Fourier series [26]. For simplicity, the following analysis adopts a simple sinusoidal function, *i.e.*, $\mu(t) = B\sin(\omega_f t)$, in which B is the maximum perturbation amplitude and ω_f the perturbation frequency. Based on the non-homogeneous ODE Eq. (8), the analytical relationship between the resonance frequency ω_0 and perturbation frequency ω_f can be derived rigorously as follows.

Theorem 2. For an underdamped platoon, the solution to Eq. (8) is represented by

$$y(t) = y_h(t) + y_p(t) \tag{9}$$

where $y_h(t)$ is the homogeneous solution and $y_p(t)$ is a particular solution. In particular,

$$y_h(t) = \sqrt{y(0)^2 + \left(\frac{\dot{y}(0) + \xi\omega_0 y(0)}{\omega_d}\right)^2}\, e^{-\xi\omega_0 t} \sin\left(\omega_d t + \tan^{-1}\left(\frac{y(0)\omega_d}{\dot{y}(0) + \xi\omega_0 y(0)}\right)\right)$$

and

$$y_p(t) = \frac{B}{\sqrt{\left(\omega_0^2 - \omega_f^2\right)^2 + \left(2\omega_0\xi\omega_f\right)^2}} \sin\left(\omega_f t - \arctan\frac{2\xi\left(\omega_f/\omega_0\right)}{1-\left(\omega_f/\omega_0\right)^2}\right).$$

Appendix B provides proof of this Theorem. According to the closed-form solutions, $Y = B/2\omega_0\xi\omega_f$ when $\omega_0 = \omega_f$. Under this condition, the particular solution, $y_p(t)$ reaches the maximum amplitude. Namely, if perturbation frequency ω_f is equal to frequency ω_0, traffic flow would have the severest oscillation with the maximum amplitude. In the mechanical vibration system, this phenomenon is called *resonance*. The above theoretical analyses lead to the following remarks.

Remark 1. The severest oscillation of the vehicle platoon occurs when the perturbation is at the resonance frequency.

Remark 2. The damping analysis of a vehicle platoon differs from platoon (in)stability analysis. The damping intensity derived from the damping process characterizes the platoon's recovery strength against perturbation.

Remark 3. The proposed approach is general enough to be applied to analyze the vulnerability of vehicle platoons with linear or nonlinear car-following behavior.

Remark 4. Periodic or pulse perturbations can be approximated as a combination of multiple harmonic functions. Thus, these types of perturbations can be captured by $\mu(t)$ on the right-hand side of non-homogeneous ODE (8).

III. Application to a Platoon with Nonlinear Car-Following Behavior

Car-following models are commonly used to describe vehicle interactions and platoon dynamics. An overview of car-following models can be found in [27]. Linear car-following models include Pipes model, Helly's model, and Gazis–Herman–Rothery model. Nonlinear car-following models include Newell's model, optimal velocity model, and the Intelligent Driver Model (IDM). The fundamental difference between these two types of car-following models is that the nonlinear models capture a nonlinear relation with respect to changes in the equilibrium speed and space gap. This section specifies the vehicle dynamics using a nonlinear car-following model, IDM, to demonstrate the applicability of our proposed vibration-theoretic approach and enable detailed theoretical validation and experimental analyses.

Compared to linear car-following models, nonlinear car-following models are more suitable for describing the real traffic flow due to their nonlinearity and sophistication in capturing complex vehicle dynamics. This research adopts the IDM due to its advantages as follows. First, the IDM is a multi-regime model that could describe more realism than other nonlinear models when characterizing the congested traffic flow [28]. Second, the IDM ensures collision-free vehicle movements, which would not cause unrealistic acceleration/deceleration shown in other car-following models [29]. The formulation of the IDM is expressed as follows [30]:

$$\dot{v}_n(t) = a\left(1 - \left(\frac{v_n(t)}{v_0}\right)^4 - \left(\frac{s^*(v_n(t), \Delta v_n(t))}{s_n(t)}\right)^2\right) \text{ with } \tag{10}$$

$$s^*(v_n(t), \Delta v_n(t)) = s_0 + Tv_n(t) - \frac{v_n(t)\cdot\Delta v_n(t)}{2\sqrt{ab}},$$

where a represents the maximum acceleration, b the desired deceleration, v_0 the maximum speed, s^* the desired safety space gap, s_0 the minimum space gap in congestion, and T the desired time gap. In the steady state, each vehicle travels with identical velocity v^e and space gap s^e. Eq. (10) yields the uniform space gap as follows:

$$s^e(v) = \left(s_0 + Tv^e\right)\left(1 - \left(\frac{v^e}{v_0}\right)^4\right)^{-1/2}. \tag{11}$$

Nevertheless, once a perturbation occurs, the uniform space gap and speed cannot maintain. Based on Eq. (4) in Lemma 1, the inherent characteristics of a platoon with the nonlinear car-following model IDM are provided below.

$$\omega_0 = \sqrt{f_n^s}\ , \quad \xi = -\frac{1}{2}\left(f_n^v + f_n^{\Delta v}\right)\Big/\sqrt{\left|f_n^s\right|}\ , \tag{12}$$

where $f_n^s = \frac{2a}{s^e}\left(\frac{s_0+Tv^e}{s^e}\right)^2$, $f_n^v = -\frac{4a(v^e)^3}{(v_0)^4} - \frac{2aT(s_0+Tv^e)}{(s^e)^2}$, $f_n^{\Delta v} = \frac{v^e}{s^e}\sqrt{\frac{a}{b}}\frac{s_0+Tv^e}{s^e}$.

These formulas imply that, because the steady space gap is determined by steady velocity based on Eq. (11), the platoon's vulnerability or inherent oscillation frequency ω_0 is determined by vehicles' mobility characteristics, including maximum acceleration, desired time gap, and steady velocity. Besides, the value of ξ is associated with other parameters, including but not limited to desired deceleration and velocity.

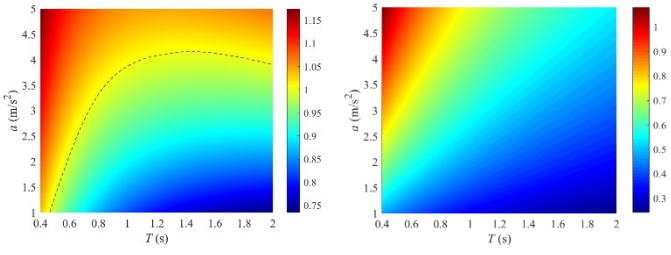

(a) Damping intensity ξ (b) Resonance frequency ω_0

Fig. 2. Damping intensity and resonance frequency variations

To articulate how damping intensity ξ and resonance frequency ω_0 are affected by different parameters, Fig. 2 depicts the variations of ω_0 and ξ with respect to a and T. Other parameters are assumed as follows: $s_0 = 2$ m, $b = 4$ m/s^2, $v_0 = 33$m/s. The color bar on the right in Fig. 2a indicates the value of ξ, and the color bar on the right in Fig. 2b indicates the value of ω_0. These figures show that the resonance frequency and damping intensity vary with parameters forming in convex surfaces for a nonlinear car-following model. The dashed line in Fig. 2a indicates the condition $\xi = 1$, which devides the region into two scenarios. Below the dashed line that means $\xi < 1$, representing that the platoon system is underdamped; otherwise, any platoon with parameters above the dashed line, *i.e.*, $\xi > 1$, represents an overdamped platoon system. As Fig. 1 has illustrated, for an underdamped system after perturbation, the distance offset fluctuates around the equilibrium state and decays gradually; while for a perturbed overdamped system, the distance offset converges to the equilibrium state quickly without overshoots.

By far, the analytical solutions to the second-order non-homogeneous ODE (8) reveal the resonance occurrence condition and explain the relationship between perturbation frequency and the vehicle platoon's oscillation patterns. In fact, our proposed method could be further extended to platoons with lane-change scenarios using models [31] beyond the scope of this study. The next section will use simulation to verify these theoretical results and further investigate the vehicle platoon vulnerability under perturbations.

IV. Simulation Study

This section presents simulation studies to demonstrate the effectiveness of the proposed vulnerability analysis approach. The platoon is composed of 10 cars. The simulation applies the IDM, Eq. (10), to update each platoon vehicle's kinematic state. All cars' velocity is set as 15m/s, and every following car's spacing gap is given by 10m. The total simulated time is 160 s. Other parameters' values are provided below: maximum velocity $v_0 = 33$ m/s, length of the car $l = 5$ m, safe space gap $s_0 = 2$ m, desired acceleration $a = 4$ m/s^2, and maximum deceleration $b = 4$ m/s^2 as suggested in [22, 32].

Our simulation considers three scenarios: no perturbations, with periodic perturbations, and the lead vehicle following a real-world vehicle trajectory. Scenario I aims to uncover the platooned vehicles' behaviors in underdamped and overdamped systems. Scenario II presents the platoon's behaviors under periodic perturbations. Scenario III applies our approach to a real-world dataset.

A. Scenario I: without perturbations

The first scenario is used as a benchmark to show the impacts of platoon's parameters on its oscillations without perturbations. As shown in Eq. (12), different parameters could generate different resonance frequencies and damping intensities. This simulation scenario contains three cases. The first case is $a = 4$m/s^2 and $T = 1$s. We can derive $\xi = 1.01 > 1$ based on Eq. (12), which indicates an overdamped system as illustrated by Fig. 3. The second case is $a = 1.5$ m/s^2 and $T = 1$ s, with corresponding $\xi = 0.86 < 1$ as illustrated by Fig. 4. The third case is $a = 1.5$ m/s^2 and $T = 1.2$ s with $\xi = 0.84 < 1$, as illustrated by Fig. 5. The last two cases indicate an underdamped system.

Fig. 3 and Fig. 4 present patterns of the platoon's dynamics for the underdamped and overdamped systems. Fig. 3 shows a rapid convergence to the equilibrium state, while Fig. 4 shows the platoon's oscillation behavior. The main difference between the two figures lies in the fluctuation amplitude. The curves of speed, and space gap in Fig. 4 have not traversed the equilibrium lines, but curves in Fig. 3 have traversed the equilibrium lines, also known as overshoots.

Moreover, Fig. 5 shows the impact of desired time gap T on the vehicle platoon dynamics after a perturbation. The vehicle platoon systems in Fig. 4 and Fig. 5 are underdamped due to ξ <1 in both cases. It can be found that the larger desired time gap would lead to a larger fluctuation amplitude and a slower recovery process to the equilibrium. Figs. 3-5 illustrate that the value of ξ is correlated to the fluctuation pattern of platoons.

The simulation results are in line with the theoretical results. The proposed vibration-theoretic approach provides such an effective measure to characterize vehicle platoon's oscillation.

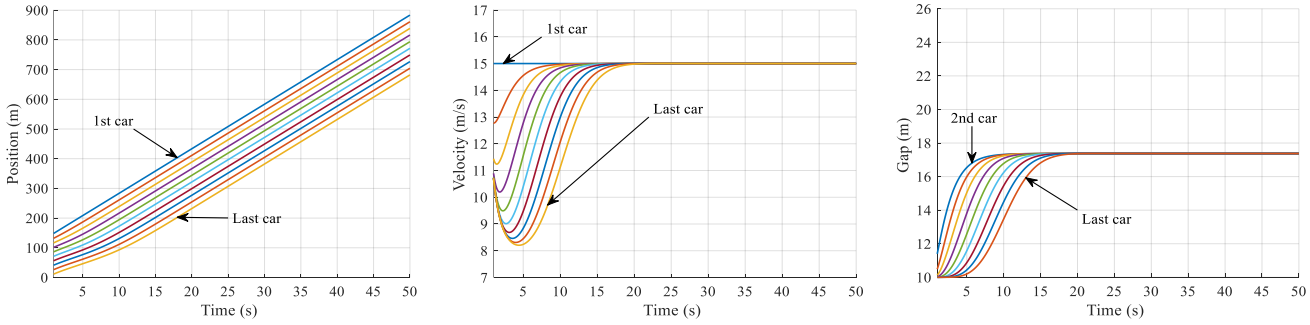

(a) Position vs. time (b) Velocity vs. time (c) Gap vs. time

Fig. 3. Plots of position, velocity, and gap variations when $a = 4$ m/s^2 and $T = 1$ s

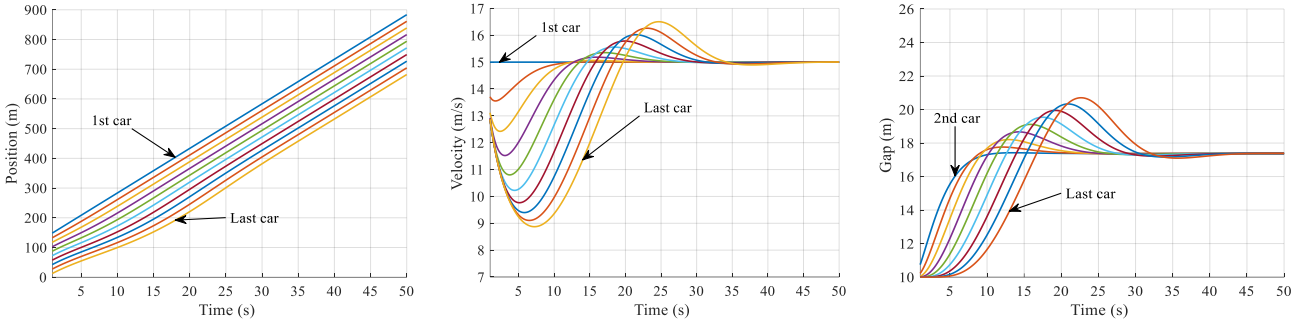

(a) Position vs. time (b) Velocity vs. time (c) Gap vs. time

Fig. 4. Plots of position, velocity, and gap variations when $a = 1.5$ m/s^2 and $T = 1$ s

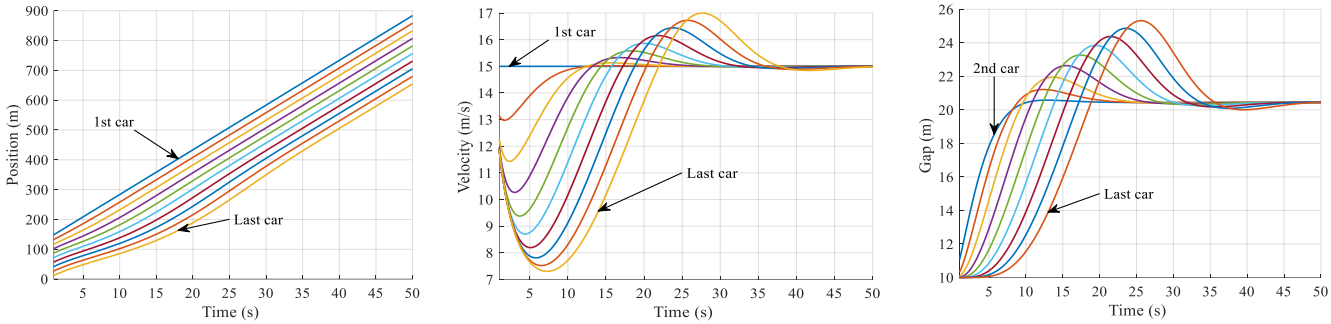

(a) Position vs. time (b) Velocity vs. time (c) Gap vs. time

Fig. 5. Plots of position, velocity, and gap variations when $a = 1.5$ m/s^2 and $T = 1.2$ s

B. Scenario II: with periodical perturbations

The second scenario focuses on the impacts of periodical perturbations on the vehicle platoon's oscillation behavior. External perturbations can influence the vehicles' behaviors through falsifying velocity, position, and acceleration messages [33, 34]. Different perturbation patterns cause different vehicles' behaviors. Without loss of generality, this simulation scenario assumes the leading vehicle's speed is perturbed in a sinusoidal fashion, *i.e.*,

$$\tilde{v}(t) = v(t) + B\sin(\omega t), \qquad (13)$$

where $\tilde{v}(t)$ is the falsified velocity, B is the maximum amplitude of the velocity deviation, and $B\sin(\omega t)$ indicates the perturbation pattern of the velocity deviation.

For comparison, same as Fig. 4, assume $a = 15$ m/s^2, $T = 1.2$ s and the initialized velocity 15 m/s. Then, the steady gap is calculated as 20.44 m based on Eq. (11). The vehicle platoon's resonance frequency can be obtained as $\omega_0 = 0.37$ rad/s. Meanwhile, the damping intensity is derived as $\xi = 0.84 < 1$, indicating a underdamped system. Assume the perturbation occurs at $t = 10$s and lasts 100 seconds.

In Fig. 6 to Fig. 8, the perturbation occurs between the two dashed lines. These three figures illustrate the impacts of different perturbation frequencies on vehicles' dynamics. In detail, Fig. 6-8 show the impacts of the perturbation frequency with $\omega = \omega_0 - 0.2 = 0.17$ $\omega = \omega_0 = 0.37$, and $\omega = \omega_0 + 0.2 = 0.57$ rad/s on vehicles' dynamics, respectively. Here, the perturbation amplitude is set as $B = 5$ m/s.

Comparing these figures, one can find that a perturbation with the resonance frequency leads to the most significant oscillations in terms of position, velocity, and gap. This phenomenon is consistent with mechanical resonance in the spring-mass system. In addition, these simulation results demonstrate that our proposed approach is meaningful and effective in revealing the vulnerability of a vehicle platoon.

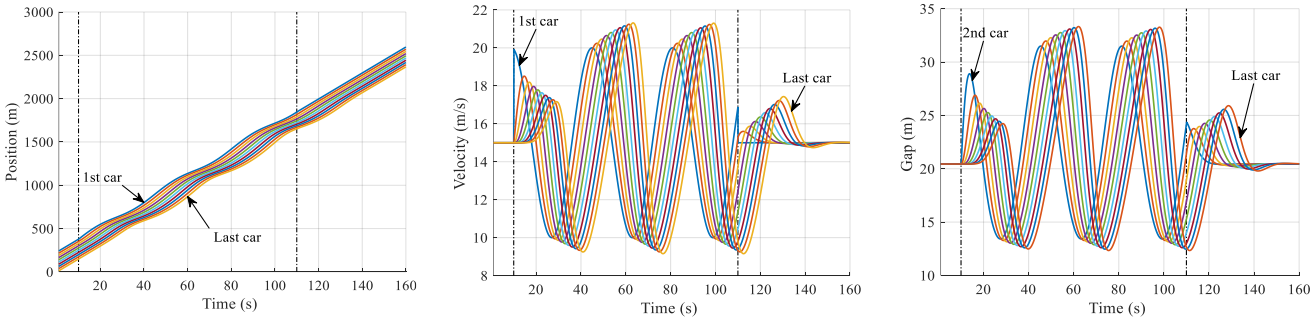

(a) Position vs. time (b) Velocity vs. time (c) Gap vs. time

Fig. 6. Impacts of perturbation frequency with $\omega = \omega_0 - 0.2 = 0.17$ rad/s on the platoon dynamics

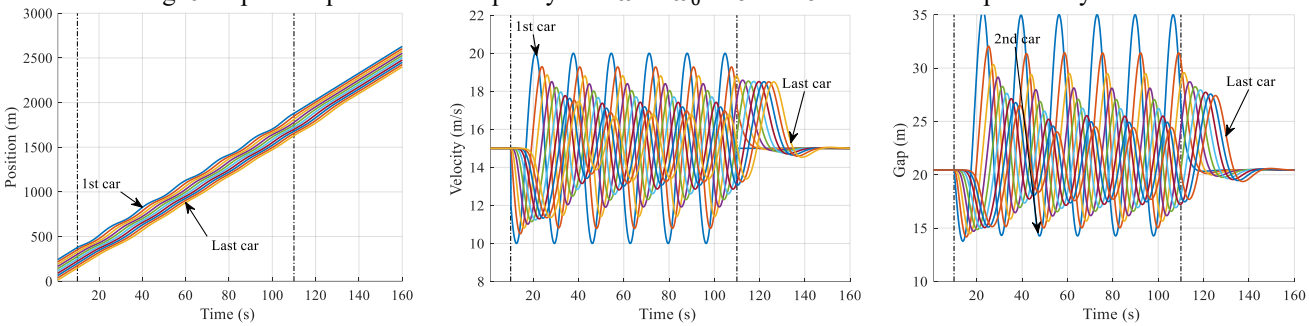

(a) Position vs. time (b) Velocity vs. time (c) Gap vs. time

Fig. 7. Impacts of perturbation frequency with $\omega = \omega_0 = 0.37$ rad/s on the platoon dynamics

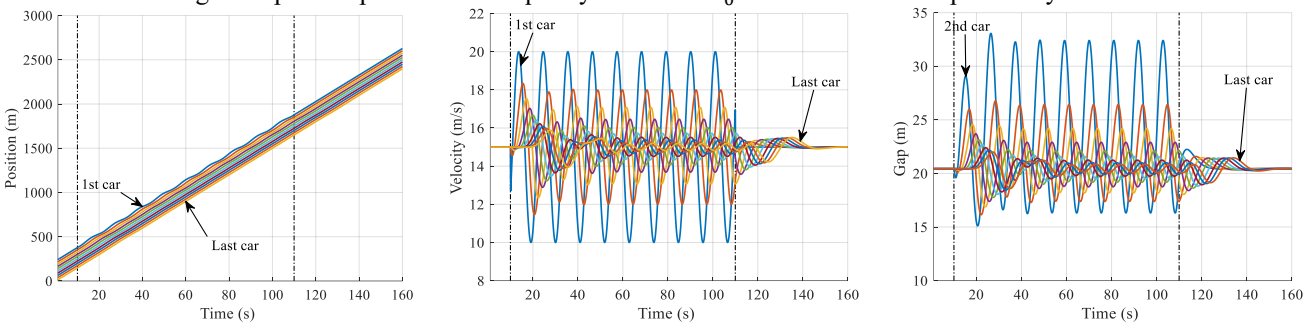

(a) Position vs. time (b) Velocity vs. time (c) Gap vs. time

Fig. 8. Impacts of perturbation frequency with $\omega = \omega_0 + 0.2 = 0.57$ rad/s on the platoon dynamics

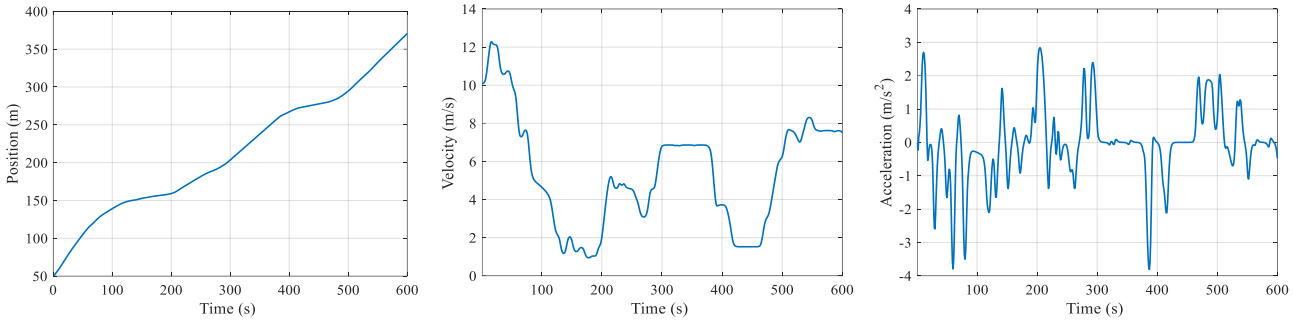

(a) Position vs. time (b) Velocity vs. time (c) Acceleration vs. time

Fig. 9 Plots of vehicle #2930 from the reconstructed NGSIM data

C. Scenario III: leading vehicle following a trajectory from the NGSIM dataset

This scenario assumes that the leading vehicle follows a practical vehicle's trajectory from the real world provided by the NGSIM dataset, which is a set of human-driven vehicle data available for traffic phenomena interpretation, parameters calibration, and theory validation [35]. Practical trajectory data used in this study are from the northbound traffic on I80 in Emeryville, California, which records from 4:00 p.m. to 4:15 p.m. on April 13, 2005, in NGSIM I80-1 dataset [36]. Our simulation adopts this data to analyze vehicles' behaviors under underdamped and overdamped conditions. The leading car adopts the practical vehicle's trajectory data and the nine following adopt the IDM platoon control strategy. Other parameters' values are same as Scenarios I and II. Note that some data quality problems including data missing, incorrect data and redundant data in the original NGSIM data. Hence, this study adopts the filtered and reconstructed data [37, 38] to mitigate the data noise. Herein, the leading vehicle uses the data of vehicle #2930 in the reconstructed dataset that shows significant undulating position, velocity, and acceleration. Vehicle #2930 is travelling in Lane 2 from 4:00 p.m. to 4:15 p.m. on April 13, 2005. This vehicle's trajectory is presented in Fig. 9.

This simulation scenario contains three cases. In the first case, $a = 5$ m/s^2 and $T = 1.6$ s. Accordingly, we can derive $\xi = 1.02 > 1$ using Eq. (12), which corresponds to an overdamped system. In the second case, $a = 5$ m/s^2, $T = 1$ s. We can derive $\xi = 0.98 < 1$ corresponding to an underdamped system. In the third case, $a = 3$ m/s^2 and $T = 0.6$ s, with $\xi = 0.89 < 1$ based on Eq. (12), which also corresponds to an underdamped platoon system.

The velocity data of the lead vehicle, illustrated in Fig. 9, clearly show that the platoon cannot travel with a constant state, and thus it can be regarded as traveling in a continuously perturbed environment. In this perturbed environment, the platoon oscillation characteristics depends heavily on the

damping intensity. When the vehicle platoon is overdamped, oscillations of the following vehicles decay over the platoon (see Fig. 10). By contrast, oscillations of the following vehicles do not decay over the string when the platoon system is underdamped. Especially, in Fig. 12, the oscillations grow over the platoon. These figures illustrate that there are serious oscillations in the underdamped vehicle platoon system but no significant oscillations appear in the overdamped vehicle platoon system when comparing Fig. 10 to Fig. 11 and Fig. 12. These results confirm that an overdamped system has stronger resistance against perturbations than an underdamped system.

Through these numerical experiments, we have verified the theoretical results derived in Section 2 and illustrated the vehicle platoon dynamics under various perturbations. The simulation results of Scenario I showed that an overdamped platoon system oscillates less than an underdamped platoon system when there is no external perturbations. Scenario II shows that resonance frequency could make the vehicle platoon oscillate the most violently. And Scenario III presents that the developed method is verified to be effective to investigate vehicle platoon's oscillation behaviors in a real-world travel environment. All these results demonstrate that the derived damping intensity is an effective tool that can well characterize the oscillations for vehicle paltoons traveling in a perturbed environment.

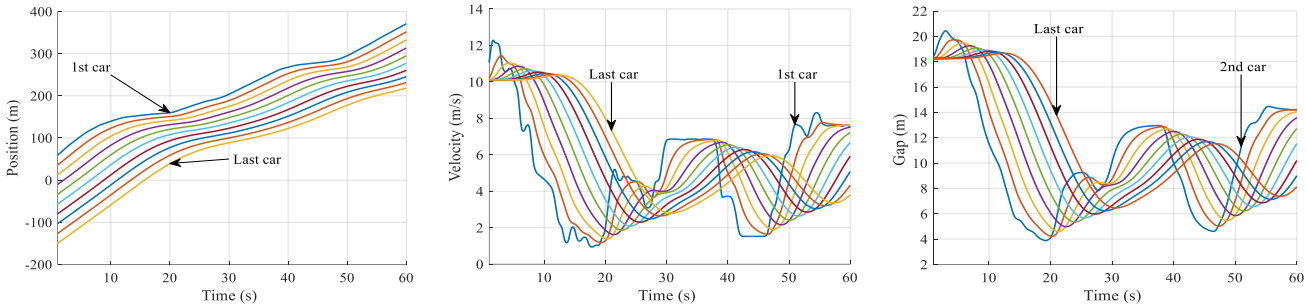

(a) Position vs. time (b) Velocity vs. time (c) Gap vs. time

Fig. 10. Plots of position, velocity, and gap variations when $a = 5\ \text{m/s}^2$ and $T = 1.6\ \text{s}$

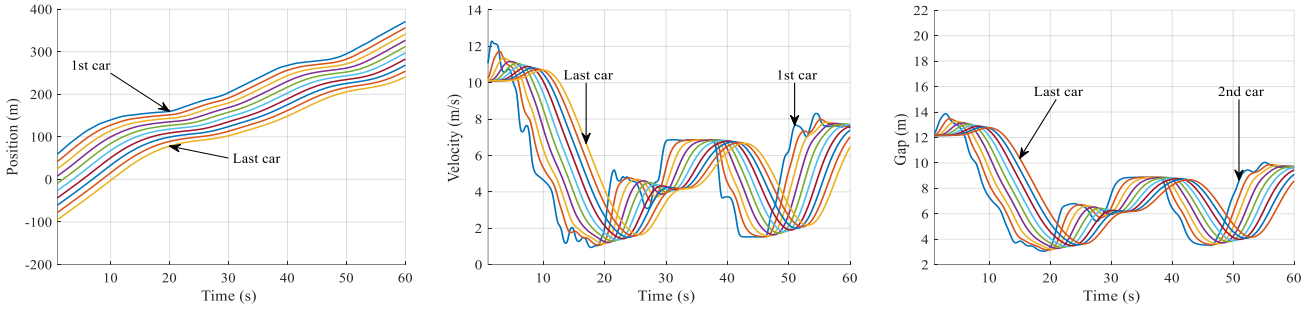

(a) Position vs. time (b) Velocity vs. time (c) Gap vs. time

Fig. 11. Plots of position, velocity, and gap variations when $a = 5\ \text{m/s}^2$ and $T = 1\ \text{s}$

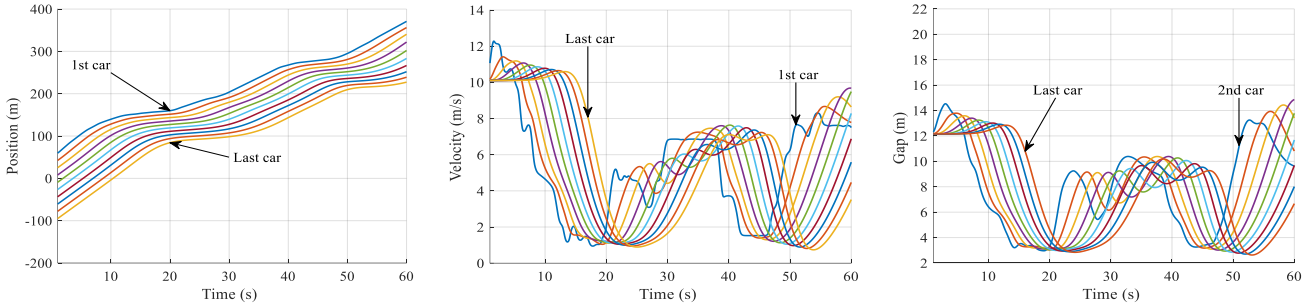

(a) Position vs. time (b) Velocity vs. time (c) Gap vs. time

Fig. 12. Plots of position, velocity, and gap variations when $a = 1.5\ \text{m/s}^2$ and $T = 1\ \text{s}$

V. Conclusions

Our research employs the mechanical vibration theory to analyze vehicle platoon vulnerability and elaborated on the vulnerability of the platoon associated with its resonance frequency and damping intensity. Simulations are carried out to verify the effectivenss of our proposed method.

Our main findings are summarized as follows. (1) This paper explores the resonance phenomena of nonlinear vehicle platoons under perturbations through rigorous theoretical analysis and proofs, leading to a closed-form formula for the oscillation amplitude under resonance. (2) A new approach has been developed that applies damping intensity to evaluate the vulnerability of vehicle platoons, by categorizing platoon

oscillations into two types: underdamped and overdamped. An overdamped system is more resilient to perturbations than an underdamped system. (3) This paper applies human-driven vehicle trajectory data from the NGSIM dataset to validate their findings through simulation. The simulation results are consistent with their theoretical analysis. (4) The analysis and simulation results suggest that perturbations with the resonance frequency can lead to the most significant oscillations. (5) Our proposed method has significant practical implications, especially for the safety of CAV systems. For example, a hacker could send a sequence of malicious messages to AVs or CAVs, leading to oscillations coinciding with platoon resonance frequency, to achieve disastrous impacts. Therefore, avoiding resonance perturbations is crucial to safeguard vehicle platoon safety and resist large amplitude oscillations.

However, there still exist some limitations of our method. For broader applications in the future, the proposed approach can be extended to incorporate complex communication topologies such as bidirectional and multiple predecessor-following types for connected automated vehicle (CAV) platoons. In particular, communication latency is an essential feature of CAV systems. Its effect on platoon vulnerability is worth an in-depth investigation. In CAV systems impacted by time-varying communication topology and/or communication latency, vehicle dynamics will change and affect the system's resonance and damping behaviors. Moreover, the proposed approach cannot used to analyze heterogeneous traffic. Future research will design innovative vehicle platooning control protocols to help heterogeneous vehicles against exerted perturbations in real-time by leveraging the findings of platoon vulnerability in this study. In addition, this study has not explained how to avoid the resonance perturbation on vehicles. There are many ways to avoid resonance perturbations. For example, applying the compensation control [39, 40] to reduce the magnitude or avoid resonance. However, developing such solutions requires another thorough study, which left for future study.

APPENDIX

A. Proof of Theorem 1

Note that the vehicle's oscillation amplitude is determined by the size of the space gap error y. It is necessary to solve the ordinary differential equation Eq. (4). Applying the characteristic equation method [41], a specific solution is obtained as follows:

$$y(t) = Ae^{st}, \tag{14}$$

where $s = i\omega$ is a Laplace variable and A is an amplitude to be determined. Take the first and second derivatives of Eq. (14) to determine the velocity and acceleration, respectively, *i.e.*,

$$\dot{y}(t) = sAe^{st} \quad \text{and} \quad \ddot{y}(t) = s^2 Ae^{st}. \tag{15}$$

Substituting Eqs. (14) and (15) into Eq (4) results in

$$s^2 Ae^{st} + 2\omega_0 \xi sAe^{st} + \omega_0^2 Ae^{st} = 0. \tag{16}$$

Grouping term gives $\left(s^2 + 2\omega_0 \xi s + \omega_0^2\right) Ae^{st} = 0$. Obviously, at least one of two terms is equivalent to zero. If $Ae^{st} = 0$, it represents there is no oscillation. Note that our focus is on investigating the vehicle platoon's oscillations, *i.e.*:

$$s^2 + 2\omega_0 \xi s + \omega_0^2 = 0. \tag{17}$$

Eq. (17) is used to obtain our fluctuation solution. We can identify the inherent oscillation frequency when the platoon oscillates. Using the quadratic formula, we can have two roots:

$$s = \left(-\xi \pm \sqrt{\xi^2 - 1}\right)\omega_0. \tag{18}$$

The form of the solution of Eq. (18) depends upon ξ. There are three possibilities depending on whether ξ is greater, less than, or equal to 1.

(i) When $\xi < 1$, the characteristic roots equation (17) becomes

$$s_1 = \left(-\xi + i\sqrt{1-\xi^2}\right)\omega_0 \quad \text{and} \quad s_2 = \left(-\xi - i\sqrt{1-\xi^2}\right)\omega_0. \tag{19}$$

Hence, the general solution of Eq. (4)is given by

$$y(t) = e^{-\xi\omega_0 t}\left(y_1 e^{it\omega_0\sqrt{1-\xi^2}} + y_2 e^{-it\omega_0\sqrt{1-\xi^2}}\right). \tag{20}$$

The underdamped motion is oscillatory with a diminishing amplitude. The inherent frequency ω_d is introduced to capture the vibration frequency of the damper system, *i.e.*,

$$\omega_d = \omega_0\sqrt{1-\xi^2}. \tag{21}$$

Furthermore, the solution of Eq. (4) can be rewritten as

$$y(t) = e^{-\xi\omega_0 t}\left(y_1 e^{i\omega_d t} + y_2 e^{-i\omega_d t}\right). \tag{22}$$

An alternative form of the solution Eq. (22) is developed by using the trigonometric identity and Euler's identity,

$$y(t) = Ae^{-\xi\omega_0 t}\sin\left(\omega_d t + \phi_d\right), \tag{23}$$

where $A = \sqrt{y(0)^2 + \left(\frac{\dot{y}(0) + \xi\omega_0 y(0)}{\omega_d}\right)^2}$, $\phi_d = \tan^{-1}\left(\frac{y(0)\omega_d}{\dot{y}(0) + \xi\omega_0 y(0)}\right)$.

(ii) When $\xi = 1$, there is only one root ω_0. This indicates a transition between the oscillatory and the aperiodic damped oscillations. Due to the repeated roots, an additional term $te^{-\xi\omega_0 t}$ is needed to keep the necessary number of arbitrary constants to satisfy both the initial conditions. Hence, the common solution is derived as

$$y(t) = \left(y_1 + y_2 t\right)e^{-\omega_0 t}, \tag{24}$$

where $y_1 = y(0)$, and $y_2 = \dot{y}(0) + \omega_0 y(0)$.

Even if the algebraic growth t, the solution still returns to its steady position as $t \to \infty$ since the exponential decay is much stronger than an algebraic growth. In this case, the perturbation of traffic flow will return to an equilibrium state in the shortest possible time without oscillation.

(iii) When $\xi > 1$, Eq. (17) has two real roots, and the motion is overdamped, *i.e.*,

$$s_1 = \left(-\xi + \sqrt{\xi^2 - 1}\right)\omega_0 \quad \text{and} \quad s_2 = \left(-\xi - \sqrt{\xi^2 - 1}\right)\omega_0. \tag{25}$$

Hence, the solution of Eq. (4) is

$$y = e^{-\xi\omega_0 t}\left(y_1 e^{t\omega_0\sqrt{\xi^2-1}} + y_2 e^{-t\omega_0\sqrt{\xi^2-1}}\right), \tag{26}$$

where $y_1 = \frac{\dot{y}(0)+\left(\xi+\sqrt{\xi^2-1}\right)\omega_0 y(0)}{2\omega_0\sqrt{\xi^2-1}}$ and $y_2 = \frac{-\dot{y}(0)-\left(\xi-\sqrt{\xi^2-1}\right)\omega_0 y(0)}{2\omega_0\sqrt{\xi^2-1}}$.

The proof of Theorem 1 is complete.

B. Proof of Theorem 2

Note that Eq. (8) is a non-homogenous ODE. According to the characteristic equation method and the superposition solution [24], the common solution of Eq. (8) can be given by

$$y(t) = y_h(t) + y_p(t) \tag{27}$$

where $y_h(t)$ is a homogeneous solution, the solution is obtained if $\mu(t) = 0$ and $y_p(t)$ is a specific solution which is specific to $\mu(t)$.

When $\mu(t) = 0$, Eq. (8) degenerates to Eq. (4). Thus, for an underdamped platoon system, the solution of Eq. (4) is equal to Eq. (5), *i.e.*,

$$y_h(t) = \sqrt{y(0)^2 + \left(\frac{\dot{y}(0)+\xi\omega_0 y(0)}{\omega_d}\right)^2}\, e^{-\xi\omega_0 t}\cdot\sin\left(\omega_d t + \tan^{-1}\left(\frac{y(0)\omega_d}{\dot{y}(0)+\xi\omega_0 y(0)}\right)\right). \tag{28}$$

When $\mu(t) = B\sin(\omega_f t) \neq 0$, $y_p(t)$ is a particular solution that is specific to $\mu(t)$. Hence, we can assume the particular solution to be of the form of

$$y_p(t) = Y\sin(\omega_f t - \phi), \tag{29}$$

where Y is the oscillation amplitude and ϕ is the displacement phase with respect to the periodic perturbation.

Substituting Eq. (29) into Eq. (8), we can derive

$$\begin{aligned}&\sin(\omega_f t)\left[\left(\omega_0^2 Y - Y\omega_f^2\right)\cos\phi + 2\omega_0\xi Y\omega_f\sin\phi - B\right]\\ &+\cos(\omega_f t)\left[-\left(\omega_0^2 Y - Y\omega_f^2\right)\sin\phi + 2\omega_0\xi Y\omega_f\cos\phi\right] = 0\end{aligned} \tag{30}$$

Because functions $\sin(\omega_f t)$ and $\cos(\omega_f t)$ are independent [42], Eq. (30) implies that

$$\begin{cases}\left(\omega_0^2 Y - Y\omega_f^2\right)\cos\phi + 2\omega_0\xi Y\omega_f\sin\phi - B = 0\\ -\left(\omega_0^2 Y - Y\omega_f^2\right)\sin\phi + 2\omega_0\xi Y\omega_f\cos\phi = 0\end{cases} \tag{31}$$

Based on Eq. (31), we have

$$\phi = \arctan\frac{2\xi\left(\omega_f/\omega_0\right)}{1-\left(\omega_f/\omega_0\right)^2} \text{ and } Y = \frac{B}{\sqrt{\left(\omega_0^2-\omega_f^2\right)^2 + \left(2\omega_0\xi\omega_f\right)^2}}.$$

The proof is complete.

REFERENCES

[1] X. Li, J. Cui, S. An, and M. Parsafard, "Stop-and-go traffic analysis: Theoretical properties, environmental impacts and oscillation mitigation," *Transportation Research Part B: Methodological, vol.* 70, pp. 319-339, 2014.

[2] M. Hu, C. Li, Y. Bian, H. Zhang, Z. Qin, and B. Xu, "Fuel Economy-Oriented Vehicle Platoon Control Using Economic Model Predictive Control," *IEEE Trans. Intell. Transp. Syst., vol.* 23, no. 11, pp. 20836-20849, 2022.

[3] D. He, T. Qiu and R. Luo, "Fuel efficiency-oriented platooning control of connected nonlinear vehicles: A distributed economic MPC approach," *Asian J. Control, vol.* 22, no. 4, pp. 1628-1638, 2020.

[4] Y. Wang, X. Li, J. Tian, and R. Jiang, "Stability Analysis of Stochastic Linear Car-Following Models," *Transp. Sci., vol.* 54, no. 1, pp. 274-297, 2020.

[5] M. Montanino, J. Monteil and V. Punzo, "From homogeneous to heterogeneous traffic flows: L_p String stability under uncertain model parameters," *Transportation Research Part B: Methodological, vol.* 146, pp. 136-154, 2021.

[6] H. Wang, X. Li, X. Zhang, J. Hu, X. Yan, and Y. Feng, "Cut through traffic like a snake: cooperative adaptive cruise control with successive platoon lane-change capability," *J. Intell. Transport. Syst.,* pp. 1-22, 2022.

[7] H. Wang, J. Lai, X. Zhang, Y. Zhou, S. Li, and J. Hu, "Make space to change lane: A cooperative adaptive cruise control lane change controller," *Transportation research part C: emerging technologies, vol.* 143, pp. 103847, 2022.

[8] A. L. Gratzer, S. Thormann, A. Schirrer, and S. Jakubek, "String Stable and Collision-Safe Model Predictive Platoon Control," *IEEE Trans. Intell. Transp. Syst., vol.* 23, no. 10, pp. 19358-19373, 2022.

[9] V. Vegamoor, S. Rathinam and S. Darbha, "String stability of connected vehicle platoons under lossy V2V communication," *IEEE Trans. Intell. Transp. Syst.,* pp. doi: 10.1109/TITS.2021.3086809, 2021.

[10] J. Monteil, M. Bouroche and D. J. Leith, "L_2 and $L\infty$ stability analysis of heterogeneous traffic with application to parameter optimization for the control of cutomated vehicles," *IEEE Trans. Control Syst. Technol., vol.* 27, no. 3, pp. 934-949, 2019.

[11] C. N. Mokogwu and K. Hashtrudi-Zaad, "Energy-Based Analysis of String Stability in Vehicle Platoons," *IEEE Trans. Veh. Technol., vol.* 71, no. 6, pp. 5915-5929, 2022.

[12] S. Feng, Y. Zhang, S. E. Li, Z. Cao, H. X. Liu, and L. Li, "String stability for vehicular platoon control: Definitions and analysis methods," *Annu. Rev. Control, vol.* 47, pp. 81-97, Mar. 2019.

[13] S. Gong, A. Zhou and S. Peeta, "Cooperative adaptive cruise control for a platoon of connected and autonomous vehicles considering dynamic information flow topology," *Transp. Res. Record, vol.* 2673, no. 10, pp. 185-198, 2019.

[14] M. R. Hajidavalloo, Z. Li, D. Chen, A. Louati, S. Feng, and W. B. Qin, "A Mechanical System Inspired Microscopic Traffic Model: Modeling, Analysis, and Validation," *IEEE T. Intell. Veh.,* pp. doi: 10.1109/TIV.2022.3146313, 2022.

[15] Y. Chen, Q. Liu, C. Wan, Q. Li, and P. Yuan, "Identification and analysis of vulnerability in traffic-intensive areas of water transportation systems," *J. Mar. Sci. Eng., vol.* 7, no. 6, pp. 174, 2019.

[16] K. Berdica, "An introduction to road vulnerability: what has been done, is done and should be done," *Transp. Policy, vol.* 9, no. 2, pp. 117-127, 2002.

[17] B. Sheehan, F. Murphy, M. Mullins, and C. Ryan, "Connected and autonomous vehicles: A cyber-risk classification framework," *Transportation Research Part A: Policy and Practice, vol.* 124, pp. 523-536, 2019.

[18] J. Ploeg, E. Semsar-Kazerooni, G. Lijster, N. van de Wouw, and H. Nijmeijer, "Graceful degradation of CACC performance subject to unreliable wireless communication," in *16th International IEEE Conference on Intelligent Transportation Systems (ITSC 2013)*, 2013, pp. 1210-1216.

[19] Z. Zhou, F. Zhu, D. Xu, S. Guo, and Y. Zhao, "Attack resilient control for vehicle platoon system with full states constraint under actuator faulty scenario," *Appl. Math. Comput., vol.* 419, pp. 126874, 2022.

[20] A. A. Shabana, *Theory of vibration: An introduction*. Chicago, IL, USA, Springer, 2019.

[21] L. A. Pipes, "An Operational Analysis of Traffic Dynamics," *J. Appl. Phys., vol.* 24, no. 3, pp. 274-281, 1953.

[22] J. Sun, Z. Zheng and J. Sun, "Stability analysis methods and their applicability to car-following models in conventional and connected environments," *Transportation Research Part B: Methodological, vol.* 109, pp. 212-237, Mar. 2018.

[23] M. Pellicer and J. Sola-Morales, "Analysis of a viscoelastic spring-mass model," *J. Math. Anal. Appl., vol.* 294, no. 2, pp. 687-698, 2004.

[24] W. Thomson, *Theory of vibration with applications*. Boca Raton, FL, USA, CRC Press, 2018.

[25] P. Wang, X. He, Y. Wei, X. Wu, and Y. Wang, "Damping behavior analysis for connected automated vehicles with linear car following control," *Transportation Research Part C: Emerging Technologies, vol.* 138, pp. 103617, 2022.

[26] G. Plonka, D. Potts, G. Steidl, and M. Tasche, *Numerical Fourier analysis*. Cham, Switzerland, Springer Nature Switzerland AG, 2018.

[27] K. Aghabayk, M. Sarvi and W. Young, "A state-of-the-art review of car-

following models with particular considerations of heavy vehicles," *Transp. Rev., vol.* 35, no. 1, pp. 82-105, Jan. 2015.
[28] A. Sarker, H. Shen, M. Rahman, M. Chowdhury, K. Dey, F. Li, Y. Wang, and H. S. Narman, "A review of sensing and communication, human factors, and controller aspects for information-aware connected and automated vehicles," *IEEE Trans. Intell. Transp. Syst., vol.* 21, no. 1, pp. 7-29, 2019.
[29] Y. Zheng, G. Zhang, Y. Li, and Z. Li, "Optimal jam-absorption driving strategy for mitigating rear-end collision risks with oscillations on freeway straight segments," *Accident Analysis & Prevention, vol.* 135, pp. 105367, 2020.
[30] M. Treiber, A. Hennecke and D. Helbing, "Congested traffic states in empirical observations and microscopic simulations," *Phys. Rev. E, vol.* 62, no. 2, pp. 1805-1824, 2000.
[31] Y. Li, C. Tang, K. Li, X. He, S. Peeta, and Y. Wang, "Consensus-based cooperative control for multi-platoon under the connected vehicles environment," *IEEE Trans. Intell. Transp. Syst., vol.* 20, no. 6, pp. 2220-2229, 2018.
[32] M. Treiber and A. Kesting, "The Intelligent Driver Model with stochasticity - New insights into traffic flow oscillations," *Transportation Research Part B: Methodological, vol.* 117, pp. 613-623, 2018.
[33] P. Wang, X. Wu and X. He, "Modeling and analyzing cyberattack effects on connected automated vehicular platoons," *Transportation Research Part C: Emerging Technologies, vol.* 115, pp. 102625, June 2020.
[34] P. Wang, G. Yu, X. Wu, Y. Wang, and X. He, "Spreading patterns of malicious information on single-lane platooned traffic in a connected environment," *Comput.-Aided Civil Infrastruct. Eng., vol.* 34, pp. 248-265, Mar. 2019.
[35] Y. Zhou, S. Ahn, M. Wang, and S. Hoogendoorn, "Stabilizing mixed vehicular platoons with connected automated vehicles: An H-infinity approach," *Transportation Research Part B: Methodological, vol.* 132, pp. 152-170, Feb. 2020.
[36] M. Montanino and V. Punzo, "On string stability of a mixed and heterogeneous traffic flow: A unifying modelling framework," *Transportation Research Part B: Methodological, vol.* 144, pp. 133-154, Feb. 2021.
[37] M. Montanino and V. Punzo, "Making NGSIM Data Usable for Studies on Traffic Flow Theory:Multistep Method for Vehicle Trajectory Reconstruction," *Transp. Res. Record, vol.* 2390, no. 1, pp. 99-111, 2013.
[38] M. Montanino and V. Punzo, "Trajectory data reconstruction and simulation-based validation against macroscopic traffic patterns," *Transportation Research Part B: Methodological, vol.* 80, pp. 82-106, 2015.
[39] L. C. Davis, "Method of compensation for the mechanical response of connected adaptive cruise control vehicles," *Physica A: Statistical Mechanics and its Applications, vol.* 562, pp. 125402, 2021.
[40] H. Xing, J. Ploeg and H. Nijmeijer, "Compensation of Communication Delays in a Cooperative ACC System," *IEEE Trans. Veh. Technol., vol.* 69, no. 2, pp. 1177-1189, 2020.
[41] R. E. O'Malley, *Singular perturbation methods for ordinary differential equations* vol. 89. New York, NY, USA, Springer-Verlag, 1991.
[42] S. G. Kelly, *Mechanical vibrations: theory and applications*. Stamford, CT, USA, Cengage Learning, 2012.

Pengcheng Wang received the Ph.D. degree in transportation from the School of Transportation Science and Engineering from Beihang University in 2020. He is an Associate Professor with the School of Cyber Science and Technology, Beihang University. His research interests include intelligent transportation systems and cybersecurity on connected vehicles.

Xinkai Wu received the Ph.D. degree from the University of Minnesota, Twin Cities, in 2010. He is currently a Professor with the School of Transportation Science and Engineering, Beihang University. His research interests include urban traffic operations, electric vehicles, and ITS. He serves as an Associate Editor for Transportation Research Part D.

Xiaozheng (Sean) He received the Ph.D. degree from the University of Minnesota, Twin Cities. He is currently an Assistant Professor with the Department of Civil and Environmental Engineering, Rensselaer Polytechnic Institute. His research areas cover transportation system modeling and simulation, interdependent infrastructure resilience, and intelligent transportation systems. He serves as an Editorial Board Member for Transportation Research Part B and a Guest Editor for several transportation journals.